Coastal exposure assessement on Bonassola bay

L. Mucerino[1a], M. Albarella[b], L. Carpi[a], G. Besio[c], A. Benedetti[d], N. Corradi[a], M. Firpo[a], M. Ferrari[a]

[a]*DISTAV Dipartimento di Scienze della Terra dell'Ambiente e della Vita, Corso Europa, 21 - 16132, Genova, Italy.*
[b]*ASIT - Ca' Foscari University of Venice, Dorsoduro 3861 - 30123 Venezia, Italy.*
[c]*DICCA Dipartimento di Ingegneria Civile etc, Via Montallegro,1 - 16132, Genova, Italy.*
[d]*CNR-ICMATE,via E. De Marini,6-16149, Genova, Italy.*

Published onOcean and Coastal Management vol 167, pp 20-31
https://doi.org/10.1016/j.ocecoaman.2018.09.015

Abstract

This paper illustrates a novel coastal vulnerability assessment approach. The approach is based on the employment of the model chain *WavewatchIII+XBeach*, which is first used to draw a vulnerability map showing the extent of the populated areas that are vulnerable to flooding, and subsequently to establish the vulnerability of the area to specific events. The model chain is calibrated by comparing the simulated runup values of a storm with those obtained by processing on-field images recorded by a camera system. The approach herein presented allows to take into account the local coastal geology features and hydrodynamics of the area so as to obtain locally accurate results. The information collected is usable by local beach managers in coastal management planning.

The method is applied on Bonassola beach, which is a micro-tidal alluvial plain located on the NW Mediterranean along the Eastern coast of Liguria, Italy. Weather and offshore waves data collected during the last 16 years were used. The application of this method has allowed to draw a map of the areas that are subject to flooding during storms and has correctly stated that three of the seven biggest storms in the last 16 years would eventually result into flooding of populated area. The study has also shown that the vulnerability of the study area to the storms is sensitive to the period and the direction of the waves.

Keywords: Coastal vulnerability runup XBeach gravel beach storms

1. Introduction

Coastal vulnerability, defined as the susceptibility of a coastal area to be affected by either inundation or erosion, affects the majority of coasts worldwide and is accountable for destruction of property and infrastructure [1].

[1]Corresponding author Luigi Mucerino (luigi.mucerino@edu.unige.it)

In the scientific literature several approaches are reported to assess coastal vulnerability and risk, that differ in complexity, in the number of processes that they include, in the possibility of application at various scales, in the accuracy of the results and in the resources that they require [2].

Coastal vulnerability can be assessed at a local or regional scale. A local scale assessment implies working at a much more detailed scale than that used by local beach managers [3], and requires details of the beach and of the coastal populated area.

Various tools are suggested to assess coastal vulnerability: index-based methods, such as the Coastal Vulnerability Index (CVI) [4], [5], [6] and its derivatives, that are very effective for an evaluation of the vulnerability on regional and large scales and also for a rough evaluation at a local scale, GIS-based decision support systems, that support decision makers in a sustainable management of natural resources and in the definition of mitigation and adaptation measures [7], and methods based on dynamic computer models that allow to integrate the time dimension in the analysis and mapping of vulnerability and risks of coastal systems to climate change [8], [9], [10], [11]. Index-based studies at a local scale mostly rely on the identification of mono-dimensional shoreline segments [4], [12], so that the information about the spatial discontinuity of hazards and vulnerability conditions at a local scale may be obscured, and misleading policy-related decisions may result [13].

Although a vast literature detailing specific system response to perturbations exists, see e.g. [14], [15], [16], only few comprehensive reviews exist that may assist coastal managers in the selection of an appropriate method for conducting a coastal vulnerability assessment [9], [17]. Also, despite wave-induced water levels are a direct threat to people, infrastructure, and ecosystems, they are not routinely included in the analysis of coastal hazards, for instance, in the weather forecasting community. In fact, due to the large number of different processes involved in coastal zones, their relative importance, and the relative highly varying spacetime dynamic characteristics, the development of an universal methodology to assess the vulnerability of coastal areas is a difficult task.

Coastal vulnerability assessments at a local scale need details on beach flooding and morphodynamic processes during storms, which are dependent on the total water level at the shoreline [18], [19]. Accurate prediction of the local wave runup height not only allows accurate vulnerability assessments and risk analysis but is also essential for the design of effective and non-intrusive coastal protection works [20] and beach nourishment projects [21], as well as for the prediction of storm wave, surge, and tsunami effects [22] and the planning of efficient coastal management schemes [23] [24] [25].

Numerical models are emerging as an effective approach in the evaluation of the storm surges induced water levels and impact on the coastline. In particu-

lar, coastal hydrodynamic and morphodynamic models, such as *XBeach*, allow to simulate a broad range of nearshore beach processes, including wave breaking, surf and swash zone processes, dune erosion, overwashing and breaching [26]. Coastal zone models, such as *SWAN* [27] and *MIKE21SW* [28] allow to simulate random, short-crested wind-generated waves in coastal regions and inland waters. Sea wave propagation models, like *WaveWatchIII* [29], [30] allow to model the generation and propagation of waves along oceans and large seas like the Mediterranean.

Model chains obtained by coupling these models allow to predict inshore water level and runup excursion at a local scale given offshore information about the meteorological conditions and wave height. Since such information can be easily gathered and to some extent predicted by modern equipment and technologies, in very recent years literature has oriented towards the employment of model chains. In [31] wave runup elevation and setup were calculated from modeled offshore wave conditions using *SWAN* and an empirical parameterizations [32] for the evaluation of coastal vulnerability and runup elevation. In [33] runup levels on Borghetto Santo Spirito Beach (Liguria, Italy) were computed by means of a model couple of *MIKE21SW* model and *Cshore* [34], a phaseaveraged cross-shore model. In [35] *SWAN* was coupled with XBeach to evaluate beach response and overwash dynamic on Santa Rosa Island during Hurricane Ivan. In [36] a model chain composed of *WaveWatchIII*, *SWAN* and *XBeach* was used to evaluate beach erosion processes induceded by hurricanes impact in Varadero (Matanzas, Cuba).

In this paper we describe a methodolgy to evaluate a bi-dimensional coastal vulnerability map on a study area along Liguria coastline, using the model chain *WaveWatchIII+XBeach* to compute runup excursion on local scale.

This work establishes a relationship between offshore climate (1999 - 2015) and coastal flooding, taking into account morphology, anthropization and hydrodynamic pattern. Offshore dataset has been provided by DICCA Meteocean hindcast (www.dicca.unige.it/meteocean/hindcast.html) spanning for the period (1979 - 2017) [37], [38]. The model chain has been validated by comparing its results with camera systems observations and employing the time stack method [39], [40], [41] to evaluate runup excursion on the images.

The most important outcome of this work consists of a Coastal Vulnerability map in which vulnerability levels are related to runup excursion induced by the most severe storms in 1999-2015. The vulnerability map highlights flooded areas of investigated area using three different vulnerability levels: urban area, beach resorts zone and bathing zone.

2. Methods

The approach followed in this work is summarized in Figure 1, and the steps are further detailed in the next Subsections.

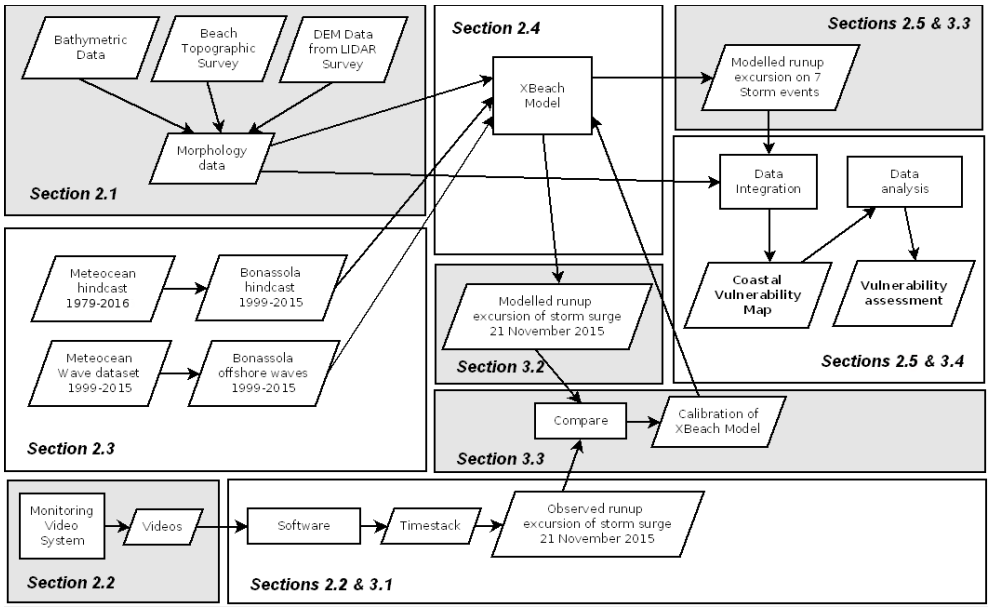

Figure 1: Overview of the workflow

2.1. Topoghaphic-bathymetric surveys and grain-size analysis

Bonassola beach, see Figure 3, is located on the Western Mediterranean sea on the eastern coast of Regione Liguria, Italy. The beach is 410 meters long, oriented NNW-SSE and lies in a small bay geographically delimited by two promontories with its backshore constrained by a promenade. Due to this morphology, the beach is totally exposed to events from SW (Mastronuzzi et al.,2017).

A complete characterization of the morphology of the study area was obtained by joining data from three different sources: bathymetric data, beach topographic surveys and a Digital Elevation Map (DEM) supplied by Regione Liguria. As shown in Figure 1 the morphology of the study area was used both for imlementing the numerical simulations and for calculating the vulnerability map.

The bathymetric data was collected using a multibeam echosounder featuring an horizontal resolution of 0.25 m, a vertical resolution of 0.006 m and an operating depth range from 0.5 m to 30 m.

Beach topographic surveys took place from 16 to 29 November 2015. Data was acquired by a DGPS with an accuracy of 0.05 m and 0.10 m on horizontal and on

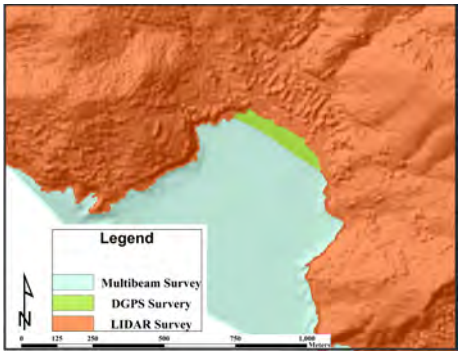

Figure 2: Surveyed area.

vertical positioning, respectively. The DEM was obtained by the LIDAR survey (2008) and is characterized by a spatial resolution of 1 m and a vertical accuracy of 1 m. According to Regione Liguria dataset (http://geoportale.regione.liguria.it) during the last 15 years, Bonassola coastline has been stable. In fact the strong embayment induced by the two promontories prevents any sediments leaks.

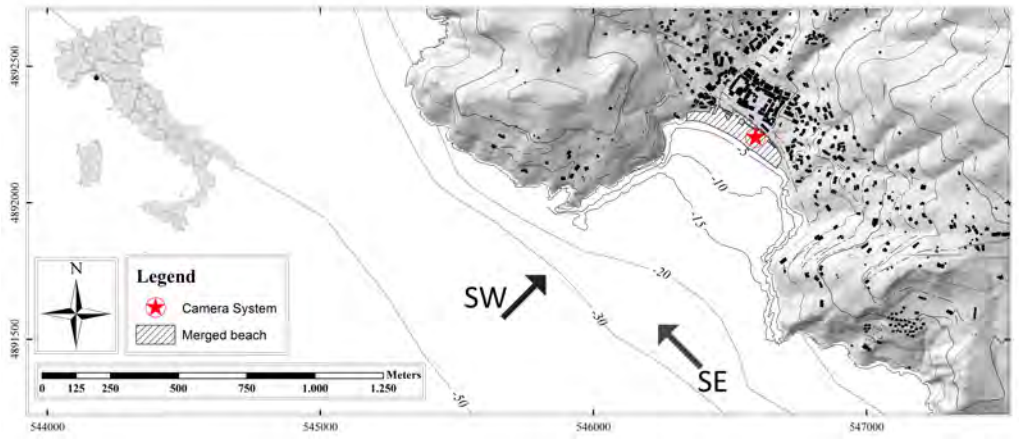

Figure 3: Study case: Bonassola bay;(★) Camera system location

Information about the grain size of the beach was taken by an analysis conducted by *University of Genoa* in 2012 and documented in [42]. The analysis was performed by dry sifting at 1/2 ϕ intervals [43]. Figure 4 shows contour mean sediment grain size and elevation of beach zone, that range, respectivily, from 0.18 mm to 30.72 mm (2.5 to -5.31 ϕ) D_{50} and from 4.5 to -20 meters depth. Based on its sediment characteristics and its morphology, Bonassola beach can be classified as Mixed Sand-Gravel beach (MSG) [44].

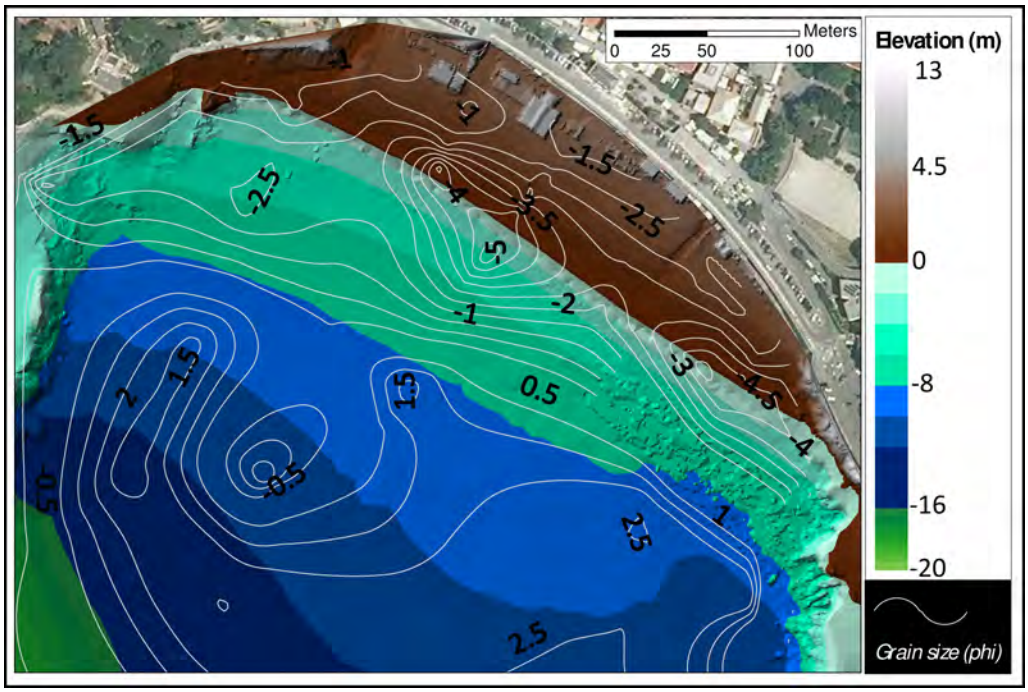

Figure 4: Grain size distribution and beach quote

2.2. Video Monitoring system

A video monitoring system including three 720x567 pixels cameras was installed at the center of Bonassola beach. The purpose of this system was to collect field data for the calibration and the validation of the numerical simulations. Cameras were installed at an elevation of about 13 m above Mean Sea Level (MSL) and their view range allowed a complete coverage of the beach, as shown in Figure 5. Camera images geo-rectification was performed by using 40 Ground Control Points (GCPs) placed in the view area of cameras: 16 on the western camera, 9 on the central camera and 15 on the eastern camera, as shown in Figure 6. The X-Y coordinates of the GCPs were acquired in UTM32-WGS84 using DGPS.

The system was used to acquire coastal images with a frame rate of 1 Hz from 19 to 24 November 2015, from 8:00 to 18:00 each day. Movies recorded by the video monitoring system were processed to derive runup values using the method of the timestack images, as suggested by extensive literature of coastal video monitoring [39], [40], [41], [45]. The runup was investigated along the three straight profiles orthogonal to the coastline in Figure 7 from 8:00 to 13:00 of 21 November 2015. As suggested by Vousdoukas [46] the horizontal position of the swash extrema was identified by using the thresholding method described

Figure 5: Bonassola camera system configuration

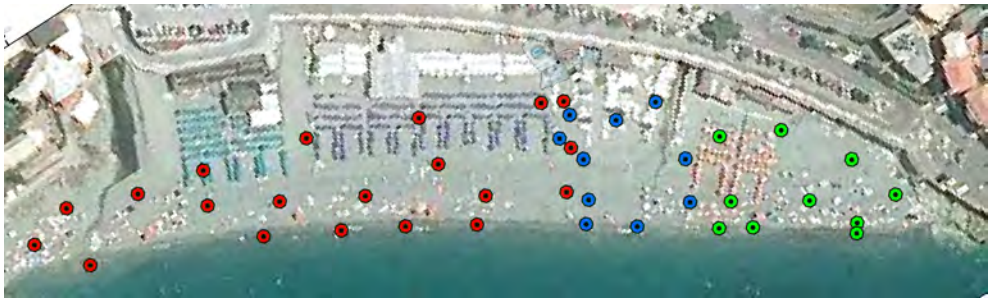

Figure 6: GCPs acquired for each Camera: western (red points), central (blue points), easter camera (green points)

by Otsu [47], and the average slope of each profile supplied by the topographic survey was used to obtain the corresponding elevation.

Analysis of the runup excursion was performed employing the 2% excedance value, $Ru_{2\%}$, and the 10% excedence value, $Ru_{10\%}$, in line with previous works [32], [48]. $Ru_{2\%}$ and $Ru_{10\%}$ were calculated on 20 minutes intervals. Image datasets were analyzed using *Beachkeeper plus* software, an image management and computing software [49].

Figure 7: Runup profile on Bonassola beach.

2.3. Offshore wave climate dataset

Offshore wave and athmospheric conditions datasets in the Mediterranean basin in the period from January 1999 to December 2015 were taken from the DICCA hindcast database by MeteOcean group (www.dicca.unige.it/meteocean/hindcast.html). This data was used to perform numerical simulations and establish the vulnerability of the beach to storm surges.

The DICCA hindcast database contains results of numerical simulations of *WaveWatchIII* [30], [29] and of the Weather Research and Forecasting (WRF-ARW) models [50] from 01/01/1979 to 31/12/2017. Validations of the hindcast resulting by the numerical simulation of the *WaveWatchIII* and *WRF-ARW* are reported in [37], [38]. For the purposes of this study, Bonassola offshore wave climate at 80 m water depth, 3.10 nautical miles off the bay was analyzed. Based on their peak wave height, the seven biggest storm surge events were collected, and their characteristic wave parameters H_s, T_p, θ_m and power spectral densities (PSD m^2/Hz) were calculated. For the Power Spectral Density the JONSWAP-type wave spectra [51] was used. The JONSWAP peak enhancement factor (γ) was set using the La Spezia buoy data (Rete Ondametrica Nazionale, RON) located about 15 nautical miles east of the study area [52].

2.4. XBeach simulations

Water levels at the shoreline in the area around Bonassola beach were modeled using *XBeach*, which is a numerical solver for coupled two-dimensional depth-averaged equations for short-wave envelope propagation and flow with spectral wave and flow boundary conditions [26]. *XBeach* was validated in [53] for predicting runup on beaches during storm surges with offshore significant wave height

in the range between 4.0 and 7.0 meters [54], [55]. An irregular mesh for *XBeach* simulations was employed, so as to obtain a higher resolution across the surf zone and a lower resolution far from the coast. The grid size was about 5 meters inshore and 25 meters offshore. The input information about the bed level was based on the combined bathymetric and topographic data described in Section 2.1. For the wave conditions at the offshore boundary, the wave climate dataset supplied by the MeteOcean group was used, as discussed in Section 2.3. Tidal data were extracted by the official Italian tide archives (http://www.mareografico.it/).

The calibration of the parameters of the XBeach model was performed as follows. As suggested in [53], hydraulic conductivity parameter (K) was set to 10 mm/s for a mixed sand-gravel beach with 12 mm (*-3.6* ϕ) median grain size (D_{50}). Groundwater level was set to 0 m and the bottom aquifer was set to 3 m below the MSL. All the other parameters were set to their recommended default value.

As suggested in [26], for extracting the runup values from simulations, the *XBeach nrugauge* module was used, which finds the last wet point before shore along a transect orthogonal to the coastline starting from a specified offshore point or *gauge point*. Table 1 and Figure 7 show the three offshore gauge points identifying the beginning of the investigated profiles in the UTM WGS84 coordinates system, using the same x-y coordinates used for profiles investigated by camera.

XBeach model was calibrated and validated for Bonassola beach by comparing along the three profiles the runup excursions obtained by simulations with those resulting by analysis of the films of the camera system during the storm surge from 8:00 to 13:00 of 21 November 2015. To this end, the obtained results by *XBeach* simulations were processed using the same methods used for the camera system. The observed runup lines were computed by processing the images recorded by the camera system with the methods described in the Section 2.2. The numerical *XBeach* runup values were obtained by performing simulations in the period 20-22 November 2015 on Bonassola beach and then by extracting the runup data along the three profiles considered for the camera system.

	UTM (E)	UTM (N)	Offshore runup gauge
East	546366	4891731	1
Center	546221	4891813	2
West	546142	4891983	3

Table 1: Offshore profile gauges used in *XBeach* model to evaluate wave runup excursions along Bonassola beach. Coordinates system used was UTM WGS84.

The comparison between the measured and the modelled runup data was restricted to the time interval 8:00 to 13:00 of 21 November 2015, during which

the camera system provided useful data. During this time interval the significant wave height H_s and the wave peak period T_p were respectively in the range 2.21-3.51 m , 9.1 - 10.5 s, and the mean wave direction θ_m was at about 231° N at seaward boundary. The calibrated model was then used to simulate the water levels on the coasts of Bonassola bay during the most severe storm surges occurred between 1999 and 2015. An analysis of the runup values along the three profiles was performed with the same methods used for the calibration. The simulation results were used for a costal vulnerability assessment further detailed in the Section 2.5. Additionally, *XBeach* simulations were used to draw a 2D map of the areas subject to flooding for each storm considered.

2.5. Coastal vulnerability

A coastal vulnerability assessment was performed for local application on Bonassola bay so as to identify areas where the implementation of measures of protection, adaptation and mitigation was necessary, and to define the respective priorities [3].

The coastal vulnerability assessment consists of two steps. In the first step, based on the results of *XBeach* simulations, a map of the areas that are likely to be flooded during the storms is drawn, on the basic assumption that zones with elevation below the maximum $Ru_{2\%}$ and contiguous to sea are flooded. The available information about the anthropization of the area is subsequently used to divide the flooded areas into three vulnerability levels with the criterion shown in Table 2, and a vulnerability map is drawn overlaying the flooded area with the color of the vulnerability level. The elevation map is used to assign to each vulnerability level a runup threshold, so that each vulnerability level is assigned an interval of runup values.

Vulnerability level	$Ru_{2\%}$ $[m]$	Legend	Flooded zone
Low	0.0 - 3.0	Green	Bathing Zone
Medium	3.0 - 4.5	Orange	Beach Resort
High	$\geq$ 4.5	Red	Builded Area

Table 2: Coastal Vulnerability legend $Ru_{2\%}$ range.

In the second step of the assessment $Ru_{2\%}$ values resulting by *XBeach* simulations described in the Section 2.4 are compared with the threshold values and the vulnerability of the area to each storm is determined.

3. Results

3.1. Camera data

Videos recorded by the system described in Section 2.2 during the storm occurred from 19 to 24 November 2015 were inspected. The most significant

events were observed in the time interval 8:00 to 13:00 of 21 November 2015, which was selected as time interval of analysis. Table 3, supplied by Meteocean, shows that during this time interval the significant wave height H_s, the wave peak period T_p and the mean wave direction θ_m were respectively in the range 2.39 m - 3.33 m, 8.70 s - 10.2 s and 229.0° - 231.6° N.

Time	H_s	T_p	θ_m
08:00 – 09:00	3.33	10.2	229.8
09:00 – 10:00	3.10	9.50	231.0
10:00 – 11:00	2.90	9.20	231.6
11:00 – 12:00	2.39	8.70	229.0
12:00 – 13:00	2.19	8.30	229.3

Table 3: Climate wave offshore conditions on 21 November 2015 in front of Bonassola bay at 80 meters depth.

Information during the time interval of analysis were processed with the methods discussed in Section 2.2. Timestack images were constructed for the three profiles shown in Figure 8, and the corresponding runup values and swash excursions were derived. Figure 8 shows the timestack image obtained by the video recorded by the east camera in the time interval from 10:00 to 11:00.

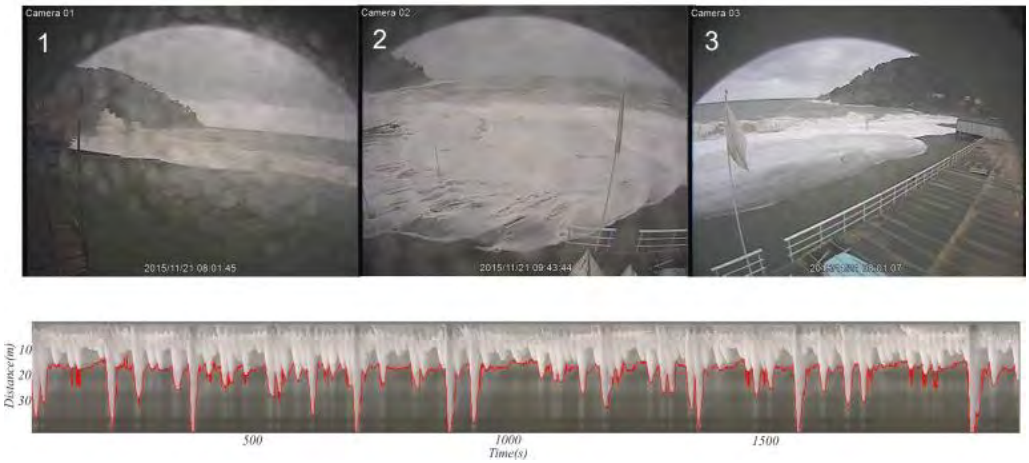

Figure 8: View of the investigated profiles from cameras. On the bottom: the timestack obtained by analyzing the videos of the east camera in the time interval from 10:00 to 11:00, highlighting with a red line the detected runup value.

Figure 9 shows the $Ru_{2\%}$ and $Ru_{10\%}$ along the three beach profiles in the time interval 8:00 to 13:00 of 21 November 2015. Wave runup peak values were recorded for all cameras at about 9:00 when a significant offshore wave height of

3.33 m and period of 10.2 s were reported.

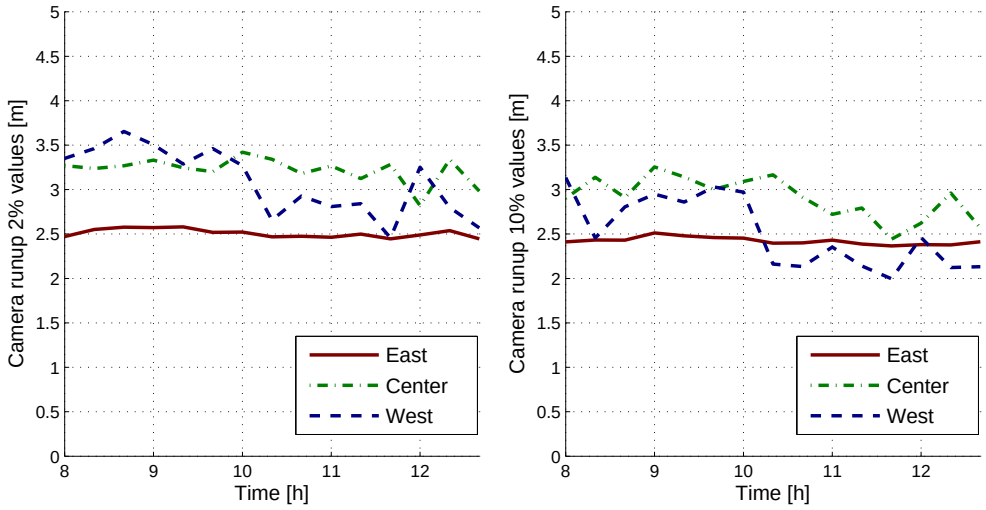

Figure 9: $Ru_{2\%}$ and$Ru_{10\%}$ as obtained by the timestack analysis on 20 minutes intervals during the time period 8:00 to 13:00 of 21 November 2015

3.2. XBeach calibration

XBeach was used to simulate the nearshore water levels in Bonassola bay during the time interval from 16:00 of 20 November to 16:00 of 21 November 2015. Figure 10 shows the offshore significant wave height and wave period during the storm as resulting by Meteocean model. The black arrow highlights the time interval in which the information obtained by the camera system and reported in Section 3.1 is available. The maximum significant wave height in front of Bonassola bay was detected at 4:00 of 21 November, with a value around 4.32 meters. The detected peak period was 10.8 seconds and the mean direction was ranging between 223° and 232° N degrees.

Runup data along the same profiles considered for the three cameras were extracted by *XBeach* numerical simulations with the methods discussed in Section 2.4. Figure 11 shows the $Ru_{2\%}$ and $Ru_{10\%}$ excedance during the time interval from 8:00 to 12:00 of 21 November.

Runup excursions obtained by numerical simulations with *XBeach* software were compared to those observed on the images recorded by the camera system. Figure 12 shows a plot of observed versus numerical $Ru_{2\%}$ and $Ru_{10\%}$ values. Numerical RMSE for $Ru_{2\%}$ and $Ru_{10\%}$ were 0.41 m and 0.27 m, thus resulting in a SCI of 0.14 and 0.10, respectively. The Relative BIASes were 0.06 and -0.01 for the$Ru_{2\%}$ and for the $Ru_{10\%}$.

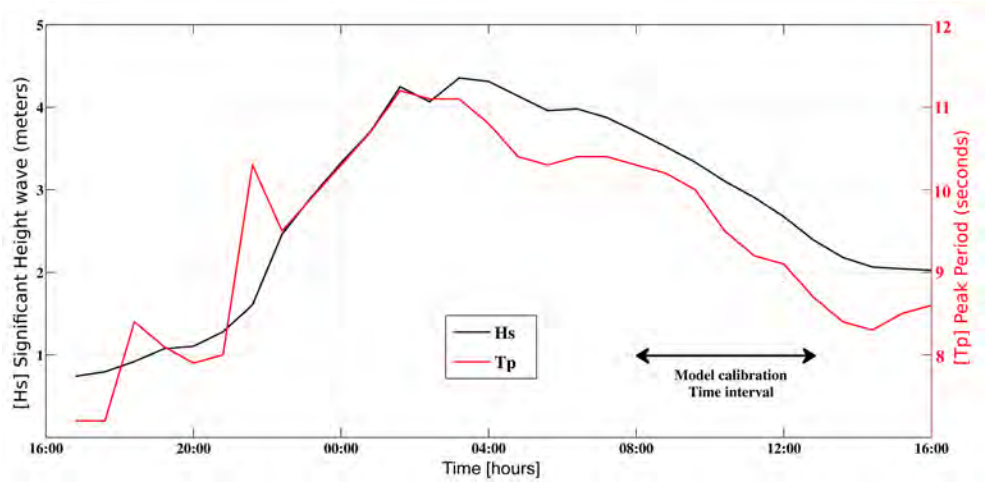

Figure 10: November 20-21, 2015 storm offshore wave height and wave period data.

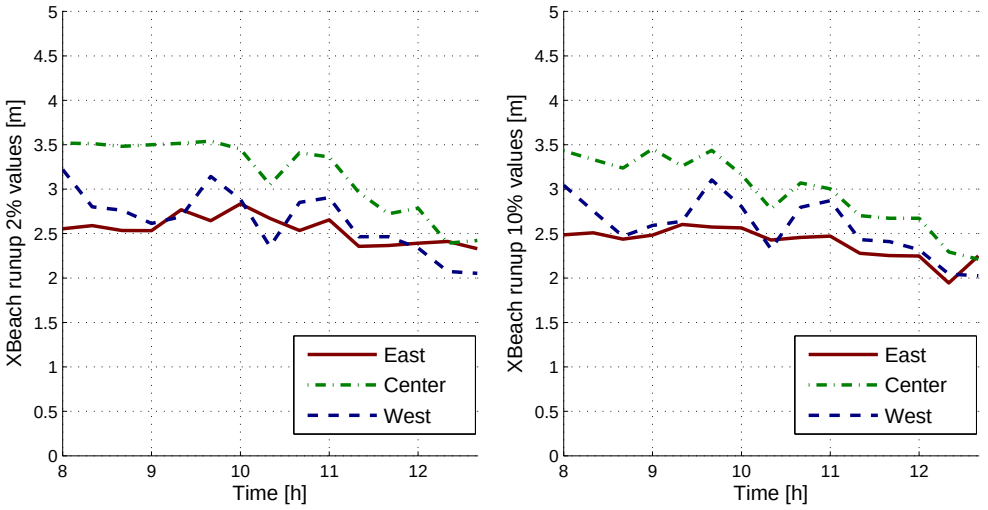

Figure 11: Runup 2% and Runup 10% as obtained by the *XBeach* simulations during the time period 8:00 to 13:00 of 21 November 2015

3.3. XBeach simulations

Based on their peak wave height the seven most severe storm surges in the years 1999-2015 were identified and their induced water levels on Bonassola beach simulated with *XBeach*. Table 4 lists the seven simulated storms together with the main characteristics of the offshore waves: energy, offshore maximum wave height, wave period and wave direction.

The calibrated and validated model was used to compute wave propagation

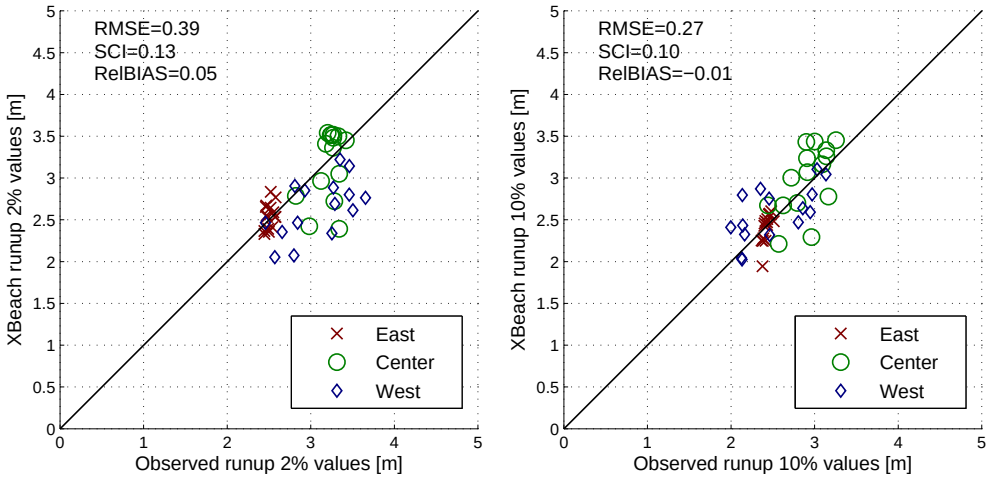

Figure 12: Left image shows comparison between observed $Ru_{2\%}$ value and modelled $Ru_{2\%}$ values;Right image shows comparison between observed $Ru_{10\%}$ value and modelled $Ru_{10\%}$ values.

Date (dd/mm/yy)	Energy [N/m^2]	H_{max} [m]	T_p [s]	Dir [$^\circ N$]	Ru_{max} [m]	$Ru_{2\%}$ [m]	$Ru_{10\%}$ [m]	Vulnerability
21/12/1999	98	6.80	11.1	228	6.15	5.96	5.60	High
06/11/2000	48	4.78	10.0	222	2.78	2.75	2.63	Low
28/05/2007	40	4.42	10.2	231	4.30	4.21	3.61	Medium
21/11/2008	135	7.74	12.2	229	6.59	6.51	5.60	High
28/10/2012	140	6.34	11.1	227	6.82	6.67	5.84	High
28/01/2015	50	5.09	10.2	229	4.25	4.19	3.72	Medium
21/11/2015	45	4.32	10.8	231	4.74	3.32	2.40	Medium

Table 4: For the seven major storms from 1999 to 2015: Offshore wave energy, wave height, wave period and wave direction, central profile maximum runup,$Ru_{2\%}$ and$Ru_{10\%}$ obtained by *XBeach* simulations and outcome of the vulnerability assessment.

and beach flooding for the seven storms considered. Simulation results were analyzed with the same methods employed for the model calibration. Figure 13 shows, for example, the runup excursion, the $Ru_{2\%}$ and the $Ru_{10\%}$ along the profile corresponding to the central camera as obtained by simulation of the storm surge in 28 October 2012.

Table 4 shows the maximum wave runup excursions and the maximum $Ru_{2\%}$ and $Ru_{10\%}$ obtained by the numerical simulations along the central profile. The maximum runup values were detected for the events in the years 1999, 2008 and 2012 with $Ru_{2\%}$, respectively, 5.96 m, 6.51 m and 6.67 m.

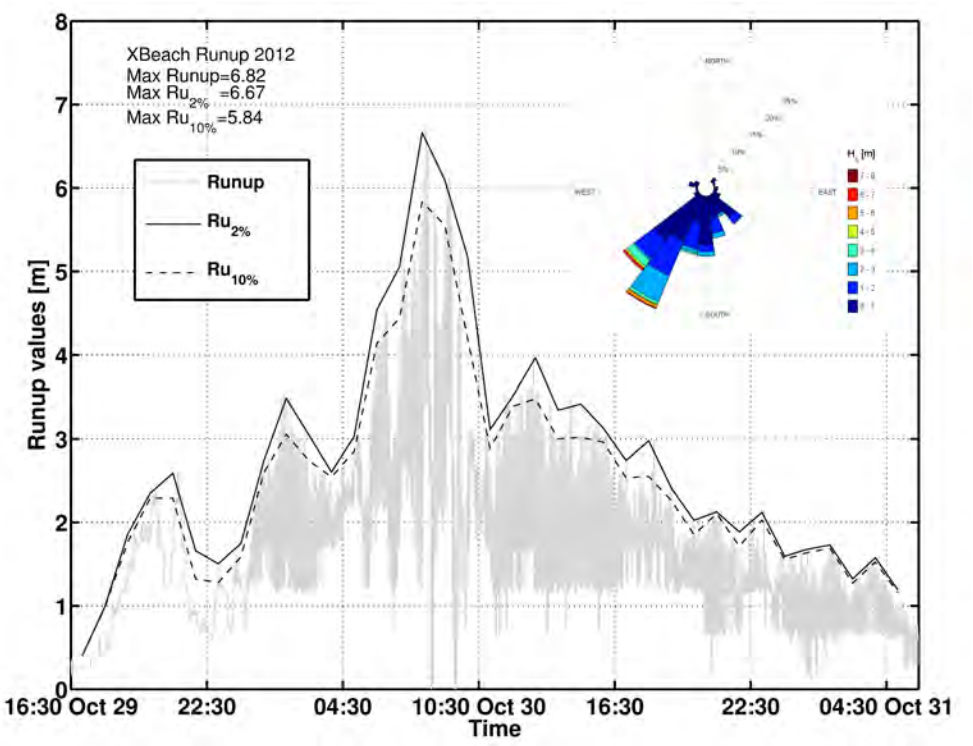

Figure 13: Wave runup, $Ru_{2\%}$ and $Ru_{10\%}$ along the profile corresponding to the central camera as obtained by simulation of the storm 29 - 31 October 2012

3.4. Coastal vulnerability assessment

Figure 14 shows the vulnerability map of Bonassola bay obtained with the methods discussed in Section 2.5.

The map shows that about 30% of the sea village is vulnerable to severe storms. The anthropic zone is protected by a bicycle overpass but flooding events may eventually occur through three gaps located on the east, the center and west side of the beach. Analyses of the data obtained by the *XBeach* simulations showed that high runup levels on the central profile result in the water eventually crossing the beach and flooding the populated area.

Table 2 reports the runup thresholds as obtained by analysis of the map.

Table 4 shows the results of the vulnerability assessment of Bonassola to each of the seven storms. The table shows that three events are classified as High Vulnerability because the $Ru_{2\%}$ runup is above 4.5 m and flooding of the builded areas is likely to occur. Offshore waves for these events are characterized by H_s between 4.32 and 7.74 meters and T_s between 10.0 and 12.2 seconds.

Three events are classified as Medium Vulnerability with $Ru_{2\%}$ ranging be-

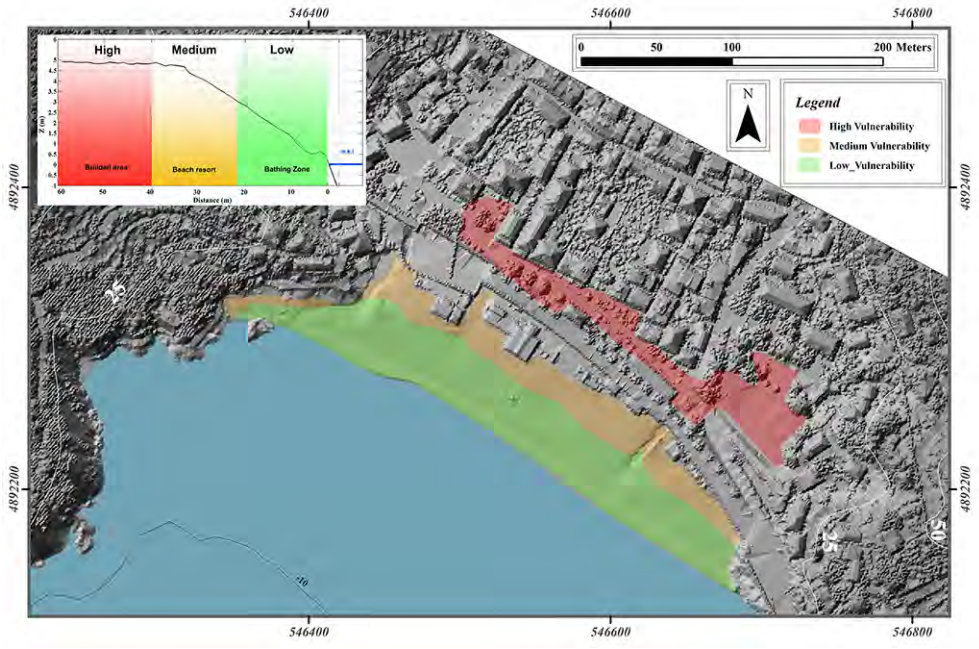

Figure 14: Map of the vulnerability on Bonassola bay; Upside on the left,application of vulnerability assement on profile

tween 3.32 and 4.21 meters and imply possibility of flooding and damage to beach structures. One event is classified as Low Vulnerability with H_s=4.78 m and T_p=10 s and a maximum $Ru_{2\%}$ of 2.75 m.

4. Discussion

Analysis of $Ru_{2\%}$ and $Ru_{10\%}$ of the Camera recorded images showed that the three profiles are subject to different water levels. Infact, at the time of the maximum recorded wave height (i.e. 8:00-9:00 of 21 November 2015), West camera showed an $Ru_{2\%}$ about 1.2 m and 0.3 m higher than that of the East and of the Center camera, respectively. Also, interestingly, $Ru_{10\%}$ is maximum for the Center camera and lower values are registered by the East camera.

These differences may be due to the different beach slope along the profiles. As described in Section 2.1, Bonassola is a mixed gravel-sand beach with variable D_{50} along the beachface. According to [44] this parameter influences beach slope and swash dynamic along the coastline. Grain size growth induces steep angle increasing due to repose angle. In details, the East profile, with a D_{50}= 30 mm (ϕ =-5) and a steeper slope, showed a lower runup excursion, while Center and West profiles, with D_{50}= 16 mm (ϕ=-4), showed higher runup results. East area

has an active profile slope of about 6.3^o while the Center and West slopes are about 4.6^o.

Comparison between *XBeach* model results and camera system data showed a good agreement. Figure 12 highlights that the best results were obtained on East and Center profiles for both the statistical values considered. Considering$Ru_{2\%}$ values, *XBeach* underestimates runup values in West profiles. This deviation may be another consequence of the non-uniform grains size distribution along Bonassola beach: in model simulation, due to the difficulties in simulating a beach with a non-uniform distribution of the grains size, an average value of 12 mm (ϕ=-3.6) was set for D_{50} parameter. *XBeach* showed more sensitive to hydraulic conductivity parameter on mixed gravel-sand beach, as the interaction between surface water and groundwater is considered to play an important role in the morphology of gravel beaches [44], [56], [57].

Vulnerability has been arranged in $High$, $Medium$ and Low based on $Ru_{2\%}$ values according to Table 4. The outcome of the vulnerability assessment has showed that the degree of vulnerability of the beach to the storms is primarily dependent on wave energy, wave height and wave peak period, with maximum coastal vulnerability associated to higher energy values, longer wave peak periods, and higher wave heigths. Yet, Table 4 shows that the area is less vulnerable to the event of November 2000 than those of November 2015 and May 2007 despite these are characterized by lower wave height, wave period and wave energy. This difference may be explained by the different direction of the waves, because the particular morphology of the coast may amplify or reduce the effects of the waves depending on their direction. These results are confirmed in the literature, for example in [1], it is suggested that the vulnerability of the area to an event may be significantly dependent by the features of the waves (H_s, T_p, Dir) and by the morphology of the area.

The outcome of the vulnerability assessment obtained by *WaveWatchIII + XBeach* simulations was partially confirmed by the residents that witnessed the effects of the storm surges under analysis. Figures 15 and 16 show damages on promenade, on turistic structures and on urban area during 2008 storm as a consequence of the flooding of the area.

The results obtained by this study suggest that a risk assessment and an evaluation of the cost effectiveness of implementing protection measures against flooding are highly recommended on this area. The vulnerability map and the vulnerability assessment give information that are useful for the risk assessment, and the evaluation of the effectiveness of some protection measures may be as well obtained by performing additional model chain simulations.

Figure 15: Damage to promenade and touristic structures after 2008 storm surge

Figure 16: Damage to urban area after 2008 storm surge

5. Conclusions

In this work an approach for assessing the coastal vulnerability to storm induced inundations has been presented, and its application on Bonassola beach has been shown. The approach is based on the employment of the *XBeach* and of the *WaveWatchIII* model for simulating the effect of offshore water levels and storms on the beach. The calibration of the model parameters was performed based on analysis of images of a Camera System with the method of the timestack images. The model was then used to simulate the effect of offshore storm induced waves on the beach. Model simulations with historical waves datasets were performed allowing to draw a vulnerability map of the area, which shows the areas that are subject to flooding during modelled storm surges, and to assess the vulnerability of the beach to each of the storms.

The main advantage of this approach is that it is suitable for a local scale assessment and that aids local coastal managers at allocating resourses for mitigating and managing damages. Infact, the model chain shows to adequately predict waves, runup excursion and coastal flooding over a small geographic area keeping into account the morphology of the area and with resolution and accuracy fine enough to aid local coastal management planning for mitigation acts. The proposed approach could provide suitable vulnerability levels on shores with different coastline orientations, grains size and beach slope.

For this approach to be employed, accurate bathymetric and topographic survey and grains size analysis are required to run the model and a camera system must be in place long enough to capture storms required for the calibration of the model. Also, since bathymetric and topographic data are subject to change over time they must be kept up to date for predictions to be accurate.

6. Acknowledgements

The authors would like to thanks *Regione Liguria - Settore Ambiente* for supplied dataset. Thanks are also given to the Municipality of Bonassola - La Spezia for logistic support. L.M., L.C., G.B., N.C., M.F., M.F. have been tended through the *Project MAREGOT* - MAnagement dei Rischi derivanti dallErosione costiera e azioni di GOvernance Transfrontaliera - Programma Interreg Italia-Francia Marittimo 2014-2020

References

[1] G. Di Paola, P. P. C. Aucelli, G. Benassai, G. Rodríguez, Coastal vulnerability to wave storms of sele littoral plain (southern italy), Natural hazards 71 (3) (2014) 1795–1819.

[2] A. Satta, M. Snoussi, M. Puddu, L. Flayou, R. Hout, An index-based method to assess risks of climate-related hazards in coastal zones: The case of tetouan, Estuarine, Coastal and Shelf Science 175 (2016) 93–105.

[3] J. Jiménez, A. Osorio, I. Marino-Tapia, M. Davidson, R. Medina, A. Kroon, R. Archetti, P. Ciavola, S. Aarnikhof, Beach recreation planning using video-derived coastal state indicators, Coastal Engineering 54 (6) (2007) 507–521.
[4] V. Gornitz, Vulnerability of the east coast, usa to future sea level rise, Journal of Coastal Research 9 (1990) 201–237.
[5] V. Gornitz, Global coastal hazards from future sea level rise, Palaeogeography, Palaeoclimatology, Palaeoecology 89 (4) (1991) 379–398.
[6] V. Gornitz, Mean sea level changes in the recent past, Climate and sea level change, observations, projections and implications (1993) 25–44.
[7] C. Mocenni, M. Casini, S. Paoletti, G. Giordani, P. Viaroli, J.-M. Z. Comenges, A Decision Support System for the management of the Sacca di Goro (Italy), Springer, 2009.
[8] J. Hinkel, R. J. Nicholls, A. T. Vafeidis, R. S. Tol, T. Avagianou, Assessing risk of and adaptation to sea-level rise in the european union: an application of diva, Mitigation and Adaptation Strategies for Global Change 15 (7) (2010) 703–719.
[9] E. Mcleod, B. Poulter, J. Hinkel, E. Reyes, R. Salm, Sea-level rise impact models and environmental conservation: A review of models and their applications, Ocean & Coastal Management 53 (9) (2010) 507–517.
[10] J. A. Warrick, D. A. George, G. Gelfenbaum, P. Ruggiero, G. M. Kaminsky, M. Beirne, Beach morphology and change along the mixed grain-size delta of the dammed elwha river, washington, Geomorphology 111 (3) (2009) 136–148.
[11] T.-J. Hsu, S. Elgar, R. Guza, Wave-induced sediment transport and onshore sandbar migration, Coastal Engineering 53 (10) (2006) 817–824.
[12] S. Torresan, A. Critto, J. Rizzi, A. Marcomini, Assessment of coastal vulnerability to climate change hazards at the regional scale: the case study of the north adriatic sea, Natural Hazards and Earth System Sciences 12 (7) (2012) 2347–2368.
[13] S. Kienberger, S. Lang, P. Zeil, Spatial vulnerability units–expert-based spatial modelling of socio-economic vulnerability in the salzach catchment, austria, Natural Hazards and Earth System Sciences 9 (3) (2009) 767–778.
[14] E. Bosom, J. Jiménez, Probabilistic coastal vulnerability assessment to storms at regional scale-application to catalan beaches (nw mediterranean), Natural hazards and Earth system sciences 11 (2) (2011) 475.
[15] G. Özyurt*, A. Ergin, Improving coastal vulnerability assessments to sea-level rise: a new indicator-based methodology for decision makers, Journal of Coastal Research (2010) 265–273.
[16] N. J. Cooper, H. Jay, Predictions of large-scale coastal tendency: development and application of a qualitative behaviour-based methodology, Journal of Coastal Research 36 (2002) 173–181.
[17] E. Ranieri, A. Hartley, A. Barbanti, F. D. Santos, A. Gomes, M. Hilden, P. Laihonen, N. Marinova, M. Santini, Methods for assessing coastal vulnerability to climate change, European Topic Centre on climate change impacts, vulnerability and adaptation (ETC CCA) technical paper, Bologna (IT) 93.
[18] A. H. Sallenger Jr, Storm impact scale for barrier islands, Journal of Coastal Research (2000) 890–895.
[19] J. A. Jiménez, A. Sancho-García, E. Bosom, H. I. Valdemoro, J. Guillén, Storm-induced damages along the catalan coast (nw mediterranean) during the period 1958–2008, Geomorphology 143 (2012) 24–33.
[20] R. Briganti, G. Bellotti, L. Franco, J. De Rouck, J. Geeraerts, Field measurements of wave overtopping at the rubble mound breakwater of rome–ostia yacht harbour, Coastal engineering 52 (12) (2005) 1155–1174.
[21] R. G. Dean, Storm damage reduction potential via beach nourishment, in: Coastal Engineering 2000, 2001, pp. 3305–3318.

[22] D. Korycansky, P. J. Lynett, Run-up from impact tsunami, Geophysical Journal International 170 (3) (2007) 1076–1088.
[23] A. Kroon, M. Davidson, S. Aarninkhof, R. Archetti, C. Armaroli, M. Gonzalez, S. Medri, A. Osorio, T. Aagaard, R. Holman, et al., Application of remote sensing video systems to coastline management problems, Coastal Engineering 54 (6) (2007) 493–505.
[24] J. J. Muñoz-Perez, B. L. de San Roman-Blanco, J. M. Gutierrez-Mas, L. Moreno, G. J. Cuena, Cost of beach maintenance in the gulf of cadiz (sw spain), Coastal Engineering 42 (2) (2001) 143–153.
[25] C. Xue, Coastal erosion and management of majuro atoll, marshall islands, Journal of Coastal Research (2001) 909–918.
[26] D. Roelvink, A. Reniers, A. Van Dongeren, J. v. T. de Vries, R. McCall, J. Lescinski, Modelling storm impacts on beaches, dunes and barrier islands, Coastal engineering 56 (11) (2009) 1133–1152.
[27] N. Booij, R. Ris, L. H. Holthuijsen, A third-generation wave model for coastal regions: 1. model description and validation, Journal of geophysical research: Oceans 104 (C4) (1999) 7649–7666.
[28] D. Mike, Spectral wave module scientific docu-mentation, Tech. rep., DHI Scientific Doe (2009).
[29] H. L. Tolman, et al., User manual and system documentation of wavewatch iii tm version 3.14, Technical note, MMAB Contribution 276 (2009) 220.
[30] G. J. Komen, L. Cavaleri, M. Donelan, K. Hasselmann, S. Hasselmann, P. Janssen, Dynamics and modelling of ocean waves, Cambridge university press, 1996.
[31] H. F. Stockdon, A. H. Sallenger, R. A. Holman, P. A. Howd, A simple model for the spatially-variable coastal response to hurricanes, Marine Geology 238 (1) (2007) 1 – 20.
[32] H. F. Stockdon, R. A. Holman, P. A. Howd, A. H. Sallenger, Empirical parameterization of setup, swash, and runup, Coastal engineering 53 (7) (2006) 573–588.
[33] E. Casella, A. Rovere, A. Pedroncini, L. Mucerino, M. Casella, L. A. Cusati, M. Vacchi, M. Ferrari, M. Firpo, Study of wave runup using numerical models and low-altitude aerial photogrammetry: A tool for coastal management, Estuarine, Coastal and Shelf Science 149 (2014) 160 – 167.
[34] N. Kobayashi, Documentation of cross-shore numerical model cshore, Center for Applied Coastal Research, University of Delaware.
[35] R. McCall, J. V. T. de Vries, N. Plant, A. V. Dongeren, J. Roelvink, D. Thompson, A. Reniers, Two-dimensional time dependent hurricane overwash and erosion modeling at santa rosa island, Coastal Engineering 57 (7) (2010) 668 – 683.
[36] A. G. Diaz, L. F. Córdova Jr, R. Lamazares, Evaluation of the beach erosion process in varadero, matanzas, cuba: Effects of different hurricane trajectories, World Academy of Science, Engineering and Technology, International Journal of Environmental, Chemical, Ecological, Geological and Geophysical Engineering 10 (5) (2016) 523–530.
[37] L. Mentaschi, G. Besio, F. Cassola, A. Mazzino, Developing and validating a forecast/hindcast system for the mediterranean sea, Journal of Coastal Research 65 (sp2) (2013) 1551–1556.
[38] L. Mentaschi, G. Besio, F. Cassola, A. Mazzino, Performance evaluation of wavewatch iii in the mediterranean sea, Ocean Modelling 90 (2015) 82–94.
[39] S. Zhang, C. Zhang, Application of ridgelet transform to wave direction estimation, Proc. of the Congress on Image and Signal Processing, Comp. Soc., Sanya, China 49 (1) (2008) 690–693.
[40] S. Takewaka, T. Nakamura, S. Misaki, Video imaging of the surf zone with moored video system, in: Proc. Coastal Eng., JSCE, Vol. 47, 2000, p. 126.
[41] C. Kuo, H.-H. Hwung, C. Chien, Using time-stack overlooking images to separate incident and reflected waves in wave flume, Wave Motion 46 (3) (2009) 189–199.

[42] I. Balduzzi, C. Cavallo, N. Corradi, M. Ferrari, L'érosion des plages de poche de la ligurie: le cas détude de bonassola (la spezia, italie), Geo-Eco-Trop 38 (1) (2014) 187–198.
[43] C. K. Wentworth, A scale of grade and class terms for clastic sediments, The Journal of Geology 30 (5) (1922) 377–392.
[44] R. Jennings, J. Shulmeister, A field based classification scheme for gravel beaches, Marine Geology 186 (3) (2002) 211–228.
[45] E. Ojeda, J. Guillén, Shoreline dynamics and beach rotation of artificial embayed beaches, Marine Geology 253 (1) (2008) 51–62.
[46] M. I. Vousdoukas, D. Wziatek, L. P. Almeida, Coastal vulnerability assessment based on video wave run-up observations at a mesotidal, steep-sloped beach, Ocean Dynamics 62 (1) (2012) 123–137.
[47] N. Otsu, A threshold selection method from gray-level histograms, Automatica 11 (285-296) (1975) 23–27.
[48] T. Poate, G. Masselink, M. Davidson, R. McCall, P. Russell, I. Turner, High frequency in-situ field measurements of morphological response on a fine gravel beach during energetic wave conditions, Marine Geology 342 (2013) 1–13.
[49] M. Brignone, C. F. Schiaffino, F. I. Isla, M. Ferrari, A system for beach video-monitoring: Beachkeeper plus, Computers & geosciences 49 (2012) 53–61.
[50] W. C. Skamarock, J. B. Klemp, A time-split nonhydrostatic atmospheric model for weather research and forecasting applications, Journal of Computational Physics 227 (7) (2008) 3465–3485.
[51] K. Hasselmann, T. Barnett, E. Bouws, H. Carlson, D. Cartwright, K. Enke, J. Ewing, H. Gienapp, D. Hasselmann, P. Kruseman, et al., Measurements of wind-wave growth and swell decay during the joint north sea wave project (jonswap), Tech. rep., Deutches Hydrographisches Institut (1973).
[52] S. Corsini, R. Inghilesi, L. Franco, R. Piscopia, Italian waves atlas, APAT-Università degli Studi di Roma 3 (2006) 134.
[53] R. McCall, G. Masselink, T. Poate, J. Roelvink, L. Almeida, M. Davidson, P. Russell, Modelling storm hydrodynamics on gravel beaches with xbeach-g, Coastal Engineering 91 (2014) 231–250.
[54] H. F. Stockdon, D. M. Thompson, N. G. Plant, J. W. Long, Evaluation of wave runup predictions from numerical and parametric models, Coastal Engineering 92 (2014) 1–11.
[55] P. Smit, G. Stelling, D. Roelvink, J. van Thiel de Vries, R. McCall, A. van Dongeren, C. Zwinkels, R. Jacobs, Xbeach: Non-hydrostatic model, Report, Delft University of Technology and Deltares, Delft, The Netherlands.
[56] T. Mason, T. Coates, Sediment transport processes on mixed beaches: a review for shoreline management, Journal of Coastal Research (2001) 645–657.
[57] D. Buscombe, G. Masselink, Concepts in gravel beach dynamics, Earth-Science Reviews 79 (1) (2006) 33–52.